



Surface soil moisture estimation over the AMMA Sahelian site in Mali using ENVISAT/ASAR data

F. Baup^{a,b,*}, E. Mougin^a, P. de Rosnay^a, F. Timouk^a, I. Chênerie^b

^a CESBIO (UPS-CNRS-CNES-IRD) 18 Avenue Edouard Belin 31401 Toulouse Cedex 9, France

^b ADMM Université Paul Sabatier 118 Route de Narbonne 31062 Toulouse Cedex 9, France

Received 10 July 2006; received in revised form 29 January 2007; accepted 29 January 2007

Abstract

This paper focuses on different methods for estimating soil moisture in a Sahelian environment by comparing ENVISAT/ASAR and ground data at the same spatial scale. The analysis is restricted to Wide Swath data in order to take advantage of their high temporal repetitivity (about 3–4 days) corresponding to a moderate spatial resolution (150 m). On the one hand, emphasis is put on the characterization of Surface Soil Moisture (SSM) at a spatial scale compatible with the derivation of the backscattering coefficients, and a transfer function is developed for up-scaling local measurements to the 1 km scale. On the other hand, three different approaches are used to normalize the angular variation of the observed backscattering coefficients. The results show a strong linear relationship between the HH normalized backscattering coefficients and SSM. The best result is obtained when restricting the ASAR data to low incidence angles and by taking into account vegetation effects using multi-angular radar data. For this case, the rms error of the SSM retrieval is 2.8%. These results highlight the capabilities of the ASAR instrument to monitor SSM in a semiarid environment.

© 2007 Published by Elsevier Inc.

Keywords: ENVISAT; ASAR; Wide Swath; Sahel; Soil moisture

1. Introduction

West Africa and more specifically the Sahelian zone has been identified by [Koster et al. \(2004\)](#) to be one among several regions of the world with the most significant feedback between soil moisture and precipitation. This hot spot “indicates where the routine monitoring of soil moisture, with both ground-based and space-based systems, will yield the greatest return in boreal summer seasonal forecasting”. Monitoring the spatial and temporal variability of soil moisture is also critical for understanding soil–vegetation–atmosphere interactions and to address the role of soil moisture on West African Monsoon dynamics ([Clark et al., 2004](#); [Monteny et al., 1997](#); [Taylor & Ellis, 2006](#); [Taylor et al., 2005](#)). Accordingly, soil moisture monitoring over the Sahel is a critical issue of the AMMA project (African Monsoon Multidisciplinary Analysis) which aims at providing a better understanding of the West African

Monsoon and its physical, chemical and biological environments ([GEWEX-news, 2006](#)).

Microwave remote sensing technology has demonstrated a quantitative ability to measure soil moisture under a variety of topographic and vegetation cover conditions. It provides spatially integrated information on soil moisture at a scale relevant for atmospheric processes and it is suitable to be extended to routine measurements from satellite systems ([Engman, 1990](#)). Several large-scale field experiments, including aircraft microwave radiometric observations, have been conducted within the framework of HAPEX, FIFE and Monsoon’90 ([Schmugge et al., 1992](#)). In semiarid regions, the relevance of aircraft L-band measurements to characterize soil moisture dynamics has been shown by [Chanzy et al. \(1997\)](#). Spaceborne systems, such as the Advanced Microwave Scanning Radiometer, AMSR-E, currently provide accurate estimates of Surface Soil Moisture (SSM) content ([Njoku et al., 2003](#)). However, only coarse spatial resolutions (> 10 km) are applicable using such methods.

Similarly, spaceborne C-band scatterometers with a high temporal sampling (4–5 days in theory) corresponding to a

* Corresponding author. CESBIO (UPS-CNRS-CNES-IRD) 18 Avenue Edouard Belin 31401 Toulouse Cedex 9, France.

E-mail address: frederic.baup@cesbio.cnes.fr (F. Baup).

spatial resolution of about 50 km have shown considerable potential for monitoring soil moisture over semiarid areas (Frison et al., 1998; Wagner & Scipal, 2000; Woodhouse & Hoekman, 2000). In particular, observations made at low incidence angles are found to be significantly related to SSM (Frison et al., 1998; Jarlan et al., 2002, 2003; Magagi & Kerr, 1997; Stephen & Long, 2004). Compared to scatterometers, Synthetic Aperture Radars (SAR) such as those onboard the European Remote Sensing (ERS) and ENVISAT satellites offer a better spatial resolution (30 m) but at the expense of a lower frequency temporal sampling (only 35 days for ENVISAT). The potential of both SAR and scatterometers for detecting changes in SSM results from their high sensitivity to the variation of the dielectric properties of the surface that are mainly linked to changes in SSM (Satalino et al., 2002; Ulaby & Batlivala, 1976; Ulaby et al., 1986; Zribi et al., 2003). Moreover, in semi-arid regions and at low incidence angles, vegetation effects are minimized or can be taken into account using relatively simple methods (Moran et al., 2000; Tansey et al., 1999). In terms of dominantly vertically-orientated herbaceous vegetation, the use of the HH polarization is expected to improve the SSM estimation from space due to the corresponding larger SSM sensitivity, especially at low incidence angle (Ulaby, 1975).

The present study focuses on examining the relationships between backscattering coefficient data acquired by the ASAR instrument at HH polarization and soil moisture measurements

recorded in a Sahelian environment. Here, only the ASAR Wide Swath data are used in order to take advantage of their high temporal sampling of 3–4 days associated with a moderate spatial resolution (150 m). The considered period is July–December 2005, which includes the entire rainy season. The paper is organized as follows: The study site, the associated data and the methodology are presented in Section 2. Three simple methods to normalize the radar data acquired at different incidence angles are described, and the interest in using LAI data for improving the angular normalization is explained. Section 3 presents the results of a correlation analysis based on the three different methods. Conclusions and Perspectives are given in Section 4.

2. Data and methods

2.1. The study site

The Agoufou (15.3°N, 1.3°W) study site is located within the AMMA meso-scale site (14.5–17.5°N, 1–2°W) in the Gourma region in Mali (Fig. 1). The Gourma region is located entirely within the Sahel bioclimatic zone and extends to the South of the Niger River between Timbuctu and Gao down to the border with Burkina-Faso. This is mainly a pastoral region enclosed by the annual average 500 and 150 mm isohyets. The rain distribution is strictly mono-modal with rainfall starting in

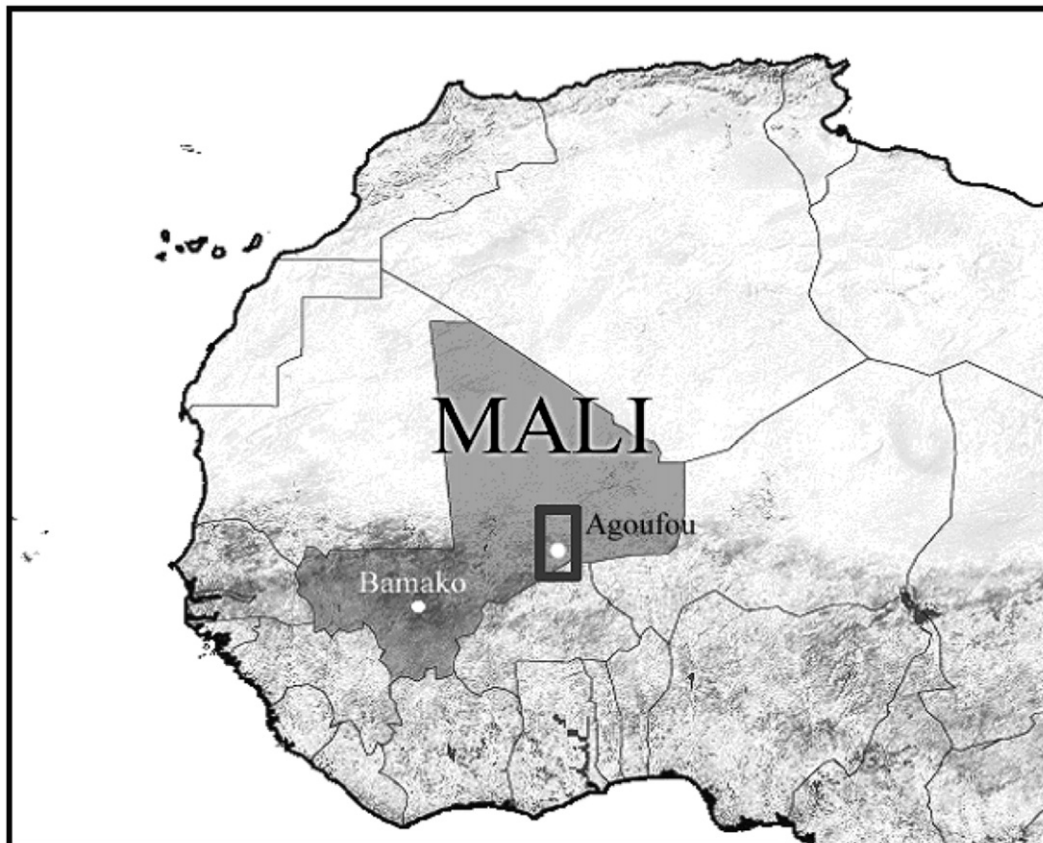


Fig. 1. The Gourma window in Mali showing the Agoufou site (●).

June and ending in September with a maximum in August. The rainy season is then followed by a long dry season characterized by the absence of green vegetation apart from some scattered trees and shrubs. Rangeland vegetation is composed of a herbaceous layer and a sparse woody plant population. Herb growth is strongly influenced by the pattern and magnitude of rainfall events and by the soil moisture regime that results from them and from run-off influenced by topography and soil texture. Annual herbs germinate after the first rains, in June or July, and unless the plants wilt before maturity owing to a lack of rainfall, the senescence coincides approximately with the end of the rainy season.

The Agoufou site ($1 \times 1 \text{ km}^2$) is a typical Sahelian landscape characterized by gently undulating sand dunes (Fig. 2). The altitude ranges between 302 and 310 meters above sea level. The total tree and shrub cover is about 4.5%, whereas the grass cover may vary from 0 to about 60% depending on soil moisture availability. The soil is coarse grained or sandy (>90%).

For the 2005 wet season, the annual rainfall total is 408 mm which can be considered as a relatively wet year (the long-term average is 370 mm). Ground measurements of the vegetation consist in an estimate of the time variation of LAI from trees and grasses using hemispherical photographs (Weiss et al., 2004). For the grass layer, a 1 km transect has been defined in the E–W direction where measurements are performed every 10 m, resulting in 100 pictures. The large quantity of data is sufficient to capture the spatial variability of the grass layer. The computed mean LAI is assumed to be representative at the 1 km^2 scale. The estimated resulting accuracy is $0.23 \text{ m}^2 \text{ m}^{-2}$ (at 1 S.D.).

In 2005, the growth of the grass layer started early in June and reached a maximum LAI of 1.8 by the end of August (Fig. 3). In contrast, the LAI of trees estimated from pictures taken of isolated individual stands remains at values lower than 0.2 throughout the year. Accordingly, trees are not considered in this study.

2.2. Surface soil moisture measurements

2.2.1. Description of the SSM measurement approach

At the Agoufou site, soil moisture measurements have been specifically designed for remote sensing applications and retrieval method validation, therefore a local soil moisture station has been installed. It covers a very fine vertical resolution in the soil, including SSM measurements at a 5 cm depth. Up-scaling features of the SSM, which are of critical importance for remote sensing, are addressed through specific SSM measurement campaigns at a 1 km spatial scale, as described herein.

The local station has been continuously measuring soil moisture and temperature profiles at a 15-min time interval since July, 2004. For soil moisture, a set of five water content reflectometers Campbell Scientific CS616 (Campbell Scientific, 2002) have been installed at 5, 10, 40, 120, 220 cm depths in the soil. Gravimetric measurements are performed for calibration of the soil moisture sensors at the local scale. The Surface Soil Moisture (SSM) is expressed in m^3/m^3 (volumetric soil water content).

In addition to the station measurements, field campaigns were conducted in order to estimate SSM at a kilometric spatial



Fig. 2. View of the Agoufou site.

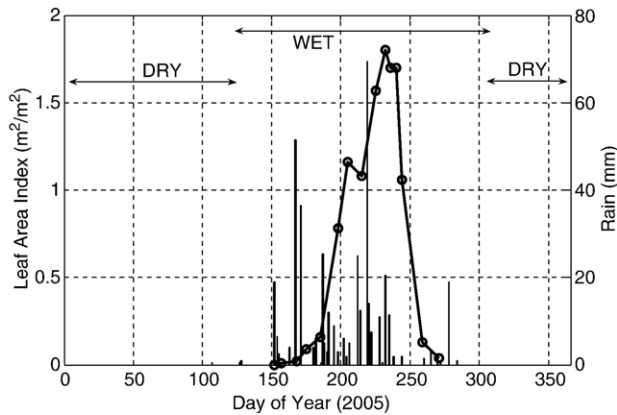


Fig. 3. Temporal evolution of the Leaf Area Index (LAI) and rainfall distribution during the 2005 wet season.

scale is expressed as a function of the local station measurements as:

$$\theta_{1 \text{ km}} = 3.945 \times \theta_{\text{Local}} - 65.51 \quad (1)$$

where (m^3/m^3) is the volumetric SSM at the 1 km scale and is the local-scale measurement (expressed here in milliseconds). Local scale measurements are kept in milliseconds in order to avoid potential calibration sensor errors.

The high correlation obtained ($r=0.97$) clearly indicates that the dynamic of the SSM at the 1 km scale is strongly correlated with the local SSM for a large range of soil moisture conditions ranging between 2% and 16%. Accordingly, this transfer function is assumed to be suitable to estimate the SSM at a 1 km scale from continuous station measurements. In the following, this relation is used to compute kilometric SSM values that are compared to ASAR data.

2.4. ENVISAT ASAR data description

The ENVISAT satellite was launched by ESA (European Space Agency) on March 1, 2002. The ASAR (Advanced Synthetic Aperture Radar) instrument is a multi-mode sensor which operates at C-band (5.3 GHz) at several polarizations (HH, VV, HV and VH), incidence angles, and spatial/radiometric resolutions depending on the functioning mode (Desnos et al., 1999). At this frequency, atmospheric perturbations can be considered negligible (Ulaby et al., 1981). The satellite passes the descending node at 10:00 a.m. local solar time and the ascending node at 22:00 p.m. with a repeat cycle of 35 days (Louet, 2001). The ASAR instrument may operate as a conventional stripmap SAR (Image and Wave modes) or as a ScanSAR (Global Monitoring, Wide Swath and Alternating Polarization modes) (Torres et al., 1999; Zink, 2002). A more detailed description of the ASAR specifications can be found in Baup et al. (2006).

In the present study, emphasis is placed on the Wide Swath (WS) mode at HH polarization. For this mode, the spatial resolution is 150 m and the incidence angles range between 16° and 43° (ENVISAT handbook, 2004). For the considered period,

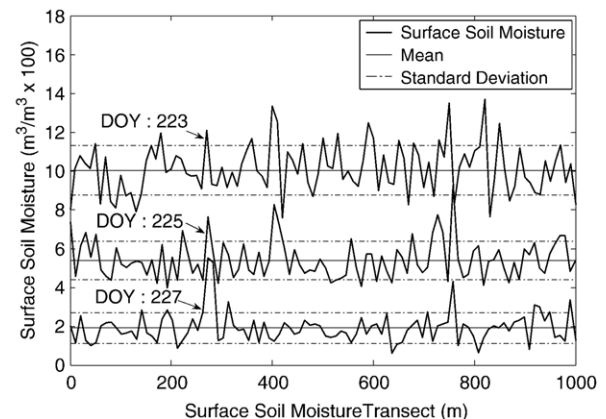


Fig. 4. Temporal Surface Soil Moisture measurements along the 1 km transect (DOY: 223, 225 and 227 of 2005) following a rainfall event on DOY 223.

scale. For this purpose, a 1 km transect was defined in the E–W direction relative to the automatic soil moisture station. Measurements are performed with a portable impedance sensor every 10 m along this transect, resulting in 100 measurements representative of the first 5 cm in the soil (Gaskin & Miller, 1996). The manufacturer calibration function for sandy soils is used to derive volumetric soil moisture values, in agreement with a gravimetric calibration performed at different locations along the transect. The mean and standard deviation (S.D.) of the 100 measurements are computed, and are assumed to be representative at the 1 km² scale. Field campaigns were conducted during the 2005 rainy season, providing a total of 25 SSM measurements for various conditions of surface soil moisture.

2.3. Up scaling local SSM to the kilometric scale

Kilometric SSM measurements are shown in Fig. 4 for Day of Year (DoY) 223, 225 and 227 (August 2005), following a 7.5 mm precipitation event on DoY 223 (August 11). For each day, the mean value and its standard deviation are represented by horizontal and dashed lines, respectively. The SSM measured on DoY 223 depicts wet conditions with values of 10.01% with a 1.28% S.D. The SSM dynamic is shown to be very pronounced with a rapid decrease of the mean SSM and standard deviation on DoY 225 (mean 5.38%, S.D. 0.99%) and 227 (mean 1.9%, S.D. 0.79%). Overall, decreases of about 2.5% per day for the 2 first days (DoY 223–225), and 1.5% per day for the 2 following days are observed. Consequently, the top soil dries out (SSM < 2%) within the 5 days following a rainfall event. The relationship between the standard deviation and mean SSM has been studied for the Agoufou site. Results show that the standard deviation increases with the mean of the SSM with a correlation of $r=0.85$. For low values of SSM (1.5%), the standard deviation is 0.8% and 2% for the highest SSM (16%). This spatial variability results from the redistribution of the water at the soil surface due to vegetation cover and topography.

In this study, transect measurements are used to estimate the relationship between SSM at the 1 km scale and the local station measurements (Fig. 5). The surface soil moisture at the 1 km

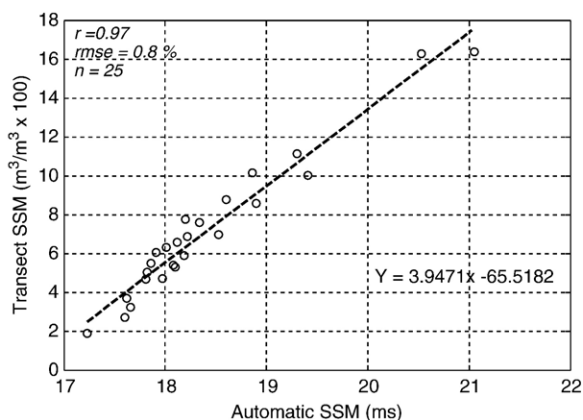


Fig. 5. Comparison between Surface Soil Moisture measurements along the 1 km transect (in %) and data collected by the automatic soil moisture station in milliseconds (July–August 2005).

from July to December, 2005, the number of available data over the Agoufou site is about 2–3 images/decade (i.e. a 10-day period), allowing the monitoring of short scale land processes such as the soil moisture variation. However, these images are acquired at different incidence angles compared to those recorded at a 35-day interval. No azimuthal difference linked to the acquisitions made during ascending or descending passes has been observed for the Agoufou site. Accordingly, in the following, data from the two different orbits are mixed together. The calibration process is performed using the B.E.S.T (Basic ENVISAT SAR Toolbox) software provided by ESA. Details on the calibration algorithm can be found in Laur et al. (1998). The geocoding is performed using the IDL/ENVI software and the results are assessed by superimposing an ASAR image onto a Landsat TM (30 m resolution). For a $1 \times 1 \text{ km}^2$ window, the estimated confidence interval for the backscattering coefficient σ^0 after angular normalization is $\pm 0.65 \text{ dB}$ (at 1σ) (Baup et al., 2006).

2.5. Methodology

Three different approaches for SSM retrieval from ASAR data are investigated in this study. The proposed approaches differ from the normalization procedure that is used to correct the angular variations of the radar signal. For the 3 considered methods, soil roughness in terms of height root mean square (hrms) and correlation length is assumed to be constant over the studied period (Jarlan et al., 2002; Wagner & Scipal, 2000). The particularity of the studied area is the low observed SSM values which range between 0.5% and 12% for the whole period under consideration. All ASAR and SSM data used are summarized in Table 1.

In the first approach, hereafter referred to as [N23], the whole ASAR data set is considered for the comparison with the SSM values. The number of available data is about 2–3 samples per decade. The approach consists of using all data acquired at various incidence angles during the dry period to establish the angular regression function which is approximated by a second order polynomial fit. Then, this function is used to normalize the entire data set at an incidence angle of 23° assuming that there is

no variation of the fit during the year. This is a reasonable assumption since the chosen incidence angle (23°) is located where the effects of vegetation are minimised. In addition, the normalization errors that result from the effects of vegetation at high incidence angles ($>30^\circ$) are expected to be small due to the low vegetation density and are thus neglected (Ulaby et al., 1982). Moreover, at a 23° incidence angle the influence of the soil roughness is also minimized (Ulaby & Batlivala, 1976; Ulaby et al., 1978; Sano et al., 1997).

The second method, [N23_season], takes into account the seasonal vegetation effect on the angular variation of the backscattered coefficient. In this case, two normalization functions depending on the season are used. For the dry season (from January to May and from October to December), which is

Table 1

Date, incidence angle, backscattering coefficient and kilometric surface soil moisture values before angular normalization of the Wide Swath ASAR data (HH polarization)

Month	Day	Time	Incidence angle ($^\circ$)	Backscattering coefficient (m^2/m^2)	Kilometric surface soil moisture ($\text{m}^3/\text{m}^3 \times 100$)
07	16	10:03:41	23.65	0.0607	5.72
07	29	09:55:09	38.04	0.0238	1.83
08	01	10:00:48	28.86	0.0618	8.56
08	05	22:17:36	39.96	0.0396	3.09
08	14	09:52:16	42.09	0.0356	3.70
08	17	09:57:56	33.65	0.0569	8.88
08	20	10:03:36	23.70	0.966	11.92
09	2	09:55:05	38.02	0.0335	6.25
09	3	22:06:13	20.83	0.0496	2.56
09	5	10:00:45	28.84	0.0282	1.87
09	6	22:11:53	31.17	0.0282	1.47
09	8	10:06:25	18.13	0.0396	1.52
09	9	22:17:34	40.03	0.0215	1.29
09	18	09:52:15	42.04	0.0204	1.14
09	21	09:57:56	33.63	0.0178	1.03
09	22	22:09:04	26.21	0.0583	3.98
09	24	10:03:36	23.68	0.0403	1.56
09	25	22:14:45	35.79	0.0232	1.03
10	7	09:54:56	38.06	0.0255	6.77
10	8	22:06:25	20.82	0.0581	3.94
10	10	10:00:36	28.86	0.0268	2.89
10	13	10:06:16	18.17	0.0623	1.69
10	14	22:17:46	40.00	0.0215	1.38
10	23	09:52:06	42.05	0.0176	1.07
10	26	09:57:47	33.61	0.0212	0.85
10	27	22:09:17	26.22	0.0327	0.76
10	29	10:03:27	23.66	0.0435	0.81
11	11	09:54:56	38.02	0.0145	0.61
11	12	22:06:25	20.85	0.0487	0.58
11	15	22:12:05	31.17	0.0194	0.56
11	17	10:06:15	18.14	0.0541	0.65
11	18	22:17:45	39.98	0.0127	0.54
11	27	09:52:02	42.07	0.0124	0.67
11	30	09:57:42	33.68	0.0163	0.65
12	1	22:09:11	26.12	0.0261	0.60
12	4	22:14:51	35.72	0.0188	0.50
12	16	09:54:50	38.06	0.0138	0.52
12	17	22:06:19	20.79	0.0458	0.41
12	19	10:00:29	28.87	0.0218	0.54
12	20	22:11:58	31.13	0.0191	0.43
12	22	10:06:09	18.16	0.0560	0.52
12	23	22:17:38	39.96	0.0120	0.47

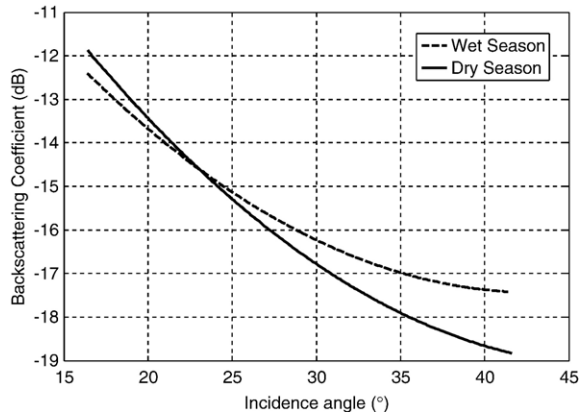


Fig. 6. Angular variations of the HH backscattering coefficient during the dry and wet seasons for the sand dune landscape estimated for the 2005 dry period and on DoY 248.

when the green vegetation cover is small or absent, the normalization function reverts to the previously established relationship [N23]. For the wet season, a simple normalization function is built by considering all of the ASAR data recorded at the date of maximum green vegetation cover. Fig. 6 illustrates the angular dependency of the radar signal during the dry (no vegetation) and the wet seasons (maximum of vegetation). The wet regression is estimated from a radar image acquired in September (DoY 248), when soil surface is getting drier and green vegetation is closed to its maximum (DoY 232). The resulting angular functions show that the effect of the vegetation layer has to be taken into account in the normalization procedure. Here, this is simply done by considering a sole ‘average’ normalization function for the whole rainy period, whatever the vegetation cover is. In contrast to previous studies (Le Hegarat-Masclé et al., 2002; Wang et al., 2004), this method does not require the use of ancillary data. The seasonal vegetation effect is simply taken into account from the seasonal analysis of the ASAR data. As for method [N23], the number of available data is about 2–3 samples per decade.

The third method [N23_season_lowangle], also considers two different regression functions depending on the season, but the data under consideration are restricted to those acquired at an incidence angle lower than 30° in order to minimize soil roughness and vegetation effects. In this case, the number of available data is about 1.2 samples per decade. At a 23° incidence angle, model simulations (Baup et al., 2006) based on the approach proposed by Karam et al. (1992), Frison et al. (1998) and Jarlan et al. (2002), indicate that the measured backscatter originates from two main contributions, namely the soil surface and the interaction between the soil and the vegetation. These contributions are mainly driven by SSM which controls the dielectric properties of the upper soil profile.

3. Surface soil moisture estimation

Relationships between SSM kilometric measurements and normalized σ^0 estimated within a $1 \times 1 \text{ km}^2$ window are examined in this section. The study is mainly performed for the Agoufou

site. The robustness of the observed relationships is measured using a correlation and root mean square error (rmse) analysis. Finally, the best inversion method is used to derive time series of SSM that are compared to the automatic kilometric-scale SSM.

3.1. Relationships between SSM and normalized σ^0

Fig. 7(a–c) illustrate the comparison between kilometric SSM and the normalized backscattering coefficients derived

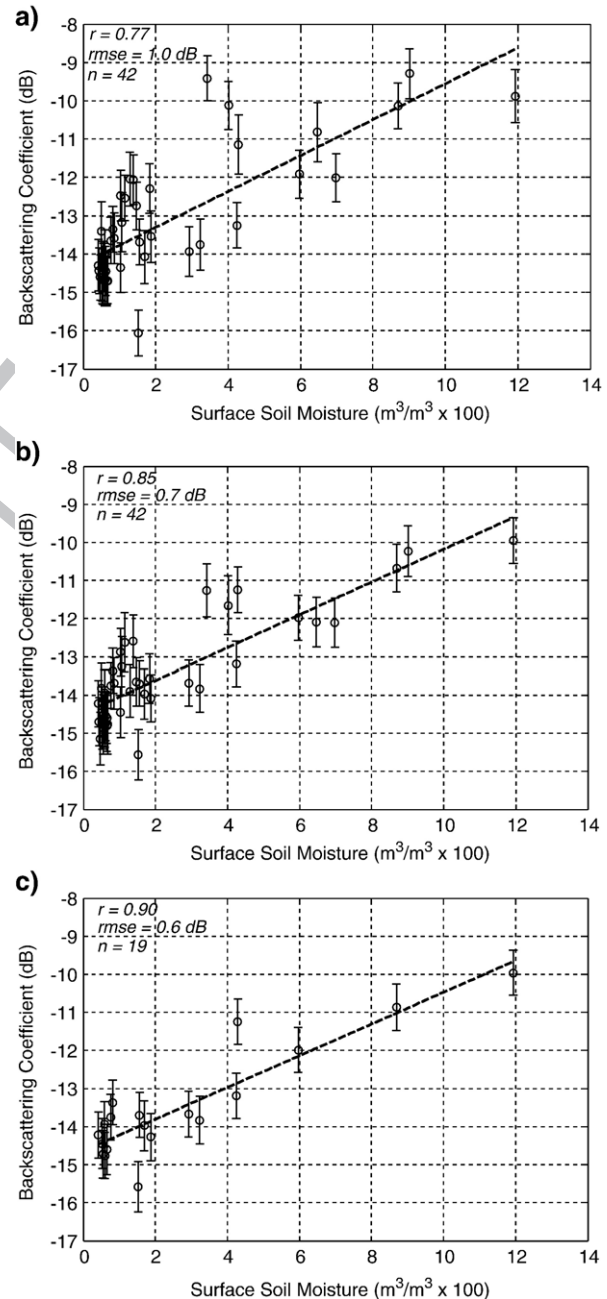


Fig. 7. a) Normalized HH backscattering coefficient versus Surface Soil Moisture for WS mode at HH Polarization (2005 rainy season). b) Normalized HH backscattering coefficient using two different functions (dry and wet season) versus the Surface Soil Moisture content for WS mode at HH Polarization. c) Normalized HH backscattering coefficient, estimated at low incidence angle (<30°), versus the Surface Soil Moisture content for WS mode at HH Polarization.

from the [N23], [N23_season] and [N23_season-lowangle] methods, respectively. For the 3 methods under consideration, results show a significant linear correlation between SSM and the normalized σ^0 , the best performance being obtained with the [N23_season-lowangle] method. Calculated correlation coefficients, r (and associated rmse in dB) are 0.77 (1.0), 0.85 (0.7), 0.90 (0.6) for the [N23], [N23_season] and [N23_season-lowangle] methods, respectively (Table 2). Whatever the method used, a large scatter in σ^0 appears especially at low SSM. Although it is related to the large amount of radar data recorded during the dry season, this large scatter is not in agreement with the observed features of SSM spatial variability (Fig. 4). Since the scatter is mainly observed during the dry season, it is assumed to be mostly related to satellite measurement noise and possible small surface roughness variations. Moreover, it is of importance to notice that the scatter of σ^0 data ranges within its normal error range (at 1σ).

3.2. Effect of seasonal vegetation dynamics on SSM estimation

For both [N23_season] and [N23_season_lowangle] methods, effects of vegetation on surface backscattering coefficient are taken into account by simply using a wet and a dry season normalization function, as depicted in Fig. 6. This method does not require any ancillary information on the vegetation status. To further investigate the effect of vegetation on soil moisture retrieval performance, seasonal features of the angular variations of the backscattering coefficient are addressed in this subsection through the use of ancillary LAI information. For each day, a sigma normalization function is interpolated between the dry and wet curves, based on a linear weighting function of the observed LAI. The corresponding date normalization function is then applied for the N23_season method, for which the whole ASAR data set is used whatever the incidence angle is. Results using this method ($r=0.83$, $\text{rmse}=1.5\%$) are similar to those obtained without LAI information ($r=0.85$, $\text{rmse}=1.4\%$).

The absence of improvement is mainly related to the low vegetation density. Accordingly, no ancillary information on LAI is used in the following.

3.3. Inverted time series of SSM

Results obtained with the [N23_season-lowangle] are presented for the July–December period, using the statistical relationship linking σ^0 and SSM, and by assuming that the minimum SSM value is 0.5%. These estimates are compared to

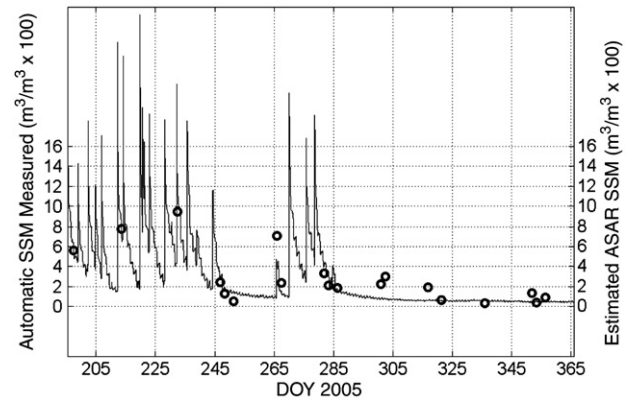


Fig. 8. Temporal variation of automatic SSM measurements and satellite-derived SSM using ASAR data acquired at low incidence angles ($<30^\circ$) for the Agoufou site (July–December 2005).

the kilometric-scale SSM measurements derived from the automatic local-scale measurements recorded at the satellite-overpass time. Results show a very good agreement between ASAR-derived SSM and SSM measurements (Fig. 8). The associated correlation coefficient is $r=0.90$ with a $\text{rmse}=1.3\%$ ($n=19$). Compared to the two other methods, the improvement is 30% and 40% in terms of rms errors of the backscattering coefficient with values of 1.0 dB, 0.7 dB and 0.6 dB for the N23, N23_season and N23_season_lowangle methods, respectively (Table 2). Similar improvement is observed when considering the rms error on the SSM from the model inversion. However, the main drawback of this method is the reduction by a factor of two of the temporal sampling.

A suitable estimate of measure errors must also take into account two other error sources:

- the confidence interval of the backscattering coefficient (± 0.6 dB) and the angular normalization error (mean equal to 0.25 dB), implying a mean radar processing error of 0.65 dB and a SSM error of 2.4%;
- the rms error due to the kilometric transfer function (0.8%).

Consequently, the resulting accuracy of the inverted SSM is 3.0%, 2.9% and 2.8% for the 3 methods, respectively, with the most significant error contribution being due to the radar accuracy (2.4%).

4. Concluding remarks

Relationships between Surface Soil Moisture, SSM, of Sahelian sandy soil and the ASAR backscattering coefficient at HH polarization are examined in this study. First, a transfer function is established for up-scaling local SSM measurements to the 1 km scale which is compatible with the ASAR estimated backscattering coefficients. Second, three radar signal angular normalization methods are tested. The proposed approaches differ in terms of the inclusion of vegetation effects in the correction. In addition, the third method is restricted to radar data which are acquired at low incidence angles in order to minimize the influence of vegetation and soil roughness.

Table 2
Comparison of the three methods in terms of correlation coefficient, rms errors (in % and in dB) and final SSM estimations errors

		r	σ^0 rmse	SSM rmse	Final SSM error (with radar errors (2.4%) and up-scaling SSM function (0.8%))
t2.4	N23	0.77	1.0 dB	1.7%	3.0%
t2.5	N23_season	0.85	0.7 dB	1.4%	2.9%
t2.6	N23_season_lowangle	0.90	0.6 dB	1.3%	2.8%

Results show a strong linear relationship between SSM and HH normalized backscattering coefficients indicating the high capabilities of the ASAR instrument to estimate SSM in a semiarid environment even at very low SSM (ranged between 0.5% and 12%). Whereas studies based on SSM estimation using SAR data in semiarid rangelands generally deal with an increased range of SSM values (up to 30% larger) and do not indicate a significant relationship for low SSM ($<15^\circ$) (Mattia et al., 2006; Moran et al., 2000). Results also clearly demonstrate that the vegetation effects have to be taken into account in order to improve the angular normalization procedure. These effects can be corrected using only multi-angular ASAR data, and the use of LAI data is not necessary for low LAI <2.0 . Although the vegetation effects are not perfectly known, especially at high incidence angles, the N23_method presented in this paper gives preliminary quantitative results, and the rms error of the Surface Soil Moisture retrieval is 2.9%. By considering only the data acquired at an incidence angle lower than 30° , the rms error is slightly reduced to 2.8%. This small improvement is obtained because the main error source comes from the σ^0 confidence interval (2.4%). Moreover, the last method reduces temporal repetitivity (1.2 data samples per decade compared to 2.8) and it would be of interest to retain the highest temporal sampling of SSM while keeping a good accuracy of the SSM retrieval. This is especially important for the Sahel, where the top surface of sandy soils dries quickly after rainfall events.

5. Uncited reference

ENVISAT ASAR product handbook, 2004

Acknowledgements

This work was performed within the framework of the AMMA project. Based on a French initiative, AMMA has been constructed by an international group and is currently funded by large number of agencies, especially from France, the UK, the US and Africa. It has been the beneficiary of a major financial contribution from the European Community's Sixth Framework Research Programme. Detailed information on the scientific coordination and funding is available on the AMMA international web site (<https://www.amma-eu.org/>). The authors thank ESA for providing the ENVISAT data used in the present study (Project ID 443, E. Mougin). The authors are grateful for all the help they received during the field measurement campaigns, especially from their colleagues and collaborators from the national institute for agronomic research in Mali, the 'Institut d'Economie Rurale'. The authors also thank Aaron Boone whose suggestions helped improve an earlier draft.

References

- Baup, F., Mougin, E., Hiernaux, P., Lopes, A., De Rosnay, P., & Ch  nerie, I. (2006). Radar signatures of Sahelian surfaces in Mali using ENVISAT-ASAR data. *IEEE Transactions on Geoscience and Remote Sensing* (in revision).
- Campbell Scientific. (2002). *CS616 Water Content Reflectometer*. User guide, Issued 6.3.02.

- Chanzy, A., Schmugge, T. J., Calvet, J. -C., Kerr, Y., Oevelen, P. V., Grosjean, O., et al. (1997). Airbone microwave radiometry on a semiarid area during HAPEX-Sahel. *Journal of Hydrology*, 188–189, 285–309.
- Clark, D. B., Taylor, C. M., & Thorpe, A. J. (2004). Feedback between the land surface and rainfall at convective length scales. *Journal of Hydrometeorology*, 5, 625–639.
- Desnos, Y. L., Laur, H., Lim, P., Meisl, P., & Gach, T. (1999). The ENVISAT-1 advanced synthetic aperture radar processor and data products. *Geoscience and Remote Sensing Symposium, IGARSS'99, Hamburg, Germany* (pp. 1683–1685).
- Engman, E. T. (1990). Progress in microwave remote sensing of soil moisture. *Canadian Journal of Remote Sensing*, 16(3), 6–14.
- ENVISAT ASAR product handbook. (2004). *European Space Agency*. Issue 1.2.
- Frison, P. L., Mougin, E., & Hiernaux, P. (1998). Observations and interpretation of seasonal ERS-1 wind scatterometer data over Northern Sahel (Mali). *Remote Sensing of Environment*, 63, 233–242.
- Gaskin, G. J., & Miller, J. D. (1996). Measurement of soil water content using a simplified impedance measuring technique. *Journal of Agricultural Engineering Resources*, 63, 153–160.
- GEWEX-news. (2006). Global Energy and Water Cycle Experiment, special issue 'AMMA west African monsoon studies are addressing water cycle issues' 16 (1).
- Jarlan, L., Mazzega, P., Mougin, E., Lavenue, F., Marty, G., Frison, P. L., et al. (2003). Mapping of Sahelian vegetation parameters from ERS scatterometer data with an evolution strategies algorithm. *Remote Sensing of Environment*, 87, 72–84.
- Jarlan, L., Mougin, E., Frison, P. L., Mazzega, P., & Hiernaux, P. (2002). Analysis of ERS wind scatterometer time series over Sahel (Mali). *Remote Sensing of Environment*, 81, 404–415.
- Karam, M. A., Fung, A. K., Lang, R. H., & Chauhan, N. S. (1992). A microwave scattering model for layered vegetation. *IEEE Transactions on Geoscience and Remote Sensing*, 30, 767–784.
- Koster, R. D., Dirmeyer, P. A., Guo, Z., Bonan, G., Chan, E., Cox, P., et al. (2004). Regions of strong coupling between soil moisture and precipitation. *Sciences*, 305, 1038–1040.
- Laur, H., Bally, P., Meadows, P., Sanchez, J., Schaettler, B., Lopinto, E., et al. (1998). *Derivation of the backscattering coefficient so in ESA SAR products*. ESA publication, Document No: ES-TN-RS-PM-HL09 17, Issue 2, Rev. 5d.
- Le Hegarat-Mascl  , S., Zribi, M., Alem, F., Weisse, A., & Loumagne, C. (2002). Soil moisture estimation from ERS/SAR data: Toward an operational methodology. *Transactions on Geoscience and Remote Sensing*, 40, 2647–2658.
- Louet J. (2001). The Envisat Mission and System. In B. 106 (Ed.). Available: http://www.esa.int/esapub/bulletin/bullet106/bul106_1.pdf
- Magagi, R. D., & Kerr, Y. H. (1997). Retrieval of soil moisture and vegetation characteristics by use of ERS-1 wind scatterometer over arid and semiarid areas. *Journal of Hydrology*, 188–189, 361–384.
- Mattia, F., Satalino, G., Dente, L., & Pasquariello, G. (2006). Using a priori information to improve soil moisture retrieval from ENVISAT ASAR AP data in semiarid regions. *IEEE Transactions on Geoscience and Remote Sensing*, 44, 900–912.
- Monteny, B. A., Lhomme, J. P., Chehbouni, A., Troufleau, D., Amadou, M., Sicot, M., et al. (1997). The role of the Sahelian biosphere on the water and the CO2 cycle during the HAPEX-Sahel experiment. *Journal of Hydrology*, 188–189, 516–535.
- Moran, M. S., Hymer, D. C., Qi, J., & Sano, E. E. (2000). Soil moisture evaluation using-temporal synthetic aperture radar (SAR) in semiarid rangeland. *Agricultural and Forest Meteorology*, 105, 69–80.
- Njoku, E., Jackson, T., Lakshmi, V., Chan, T., & Nghiem, S. V. (2003). Soil moisture retrieval from AMSR-E. *IEEE Transactions on Geoscience and Remote Sensing*, 41(2), 215–229.
- Sano, E. E., Moran, M. S., Huete, A. R., & Miura, T. (1997). C- and multiangle Ku-band synthetic aperture radar data for bare soil moisture estimation in agricultural areas. *Remote Sensing Environment*, 64, 77–90.
- Satalino, G., Mattia, F., Davidson, M. W. J., Toan, T. L., Pasquariello, G., & Borgeaud, M. (2002). On current limits of soil moisture retrieval from ERS-SAR data. *Transactions on Geoscience and Remote Sensing*, 40, 2438–2447.
- Schmugge, T., Jackson, T., Kustas, T. J., & Wang, J. R. (1992). Passive microwave remote sensing of soil moisture: Results from HAPEX, FIFE and MONSOON'90. *ISPRS Journal of Photogrammetry and Remote Sensing*, 47, 127–143.

- Stephen, H., & Long, D. G. (2004). Analysis of scatterometer observations of Saharian ergs using a simple rough facet model. *IEEE Transactions on Geoscience and Remote Sensing, Geoscience and Remote Sensing Symposium, IGARSS'04, Proceedings, vol. 3* (pp. 1534–1537).
- Tansey, K. J., Millington, A. C., Battikhi, A. M., & White, K. H. (1999). Monitoring soil moisture dynamics using satellite imaging radar in northeastern Jordan. *Applied Geography, 19*, 325–344.
- Taylor, C. M., & Ellis, R. J. (2006). Satellite detection of soil moisture impacts on convection at the mesoscale. *Geophysical Research Letters, 33*. doi:10.1029/2005GL02525
- Taylor, C. M., Parker, D. J., Lloyd, C. R., & Thorncroft, C. D. (2005). Observations of synoptic scale land surface variability and its coupling with the atmosphere. *Quarterly Journal of the Royal Meteorological Society, 13*, 913–938.
- Torres, R., Buck, C., Guijarro, J., Suchail, J. L., & Schöenberg, A. (1999). The ENVISAT ASAR instrument verification and characterisation. *CEOS SAR Workshop, Toulouse, France*.
- Ulaby, F. T. (1975). Radar Response to vegetation. *IEEE Transaction on Antennas and Propagation, AP-23*, 36–45.
- Ulaby, F. T., & Batlivala, P. P. (1976). Optimum radar parameters for mapping soil moisture. *IEEE Transaction on Geoscience Electronics, 14*(2), 81–93.
- Ulaby, F. T., Batlivala, P. P., & Dobson, M. C. (1978). Microwave backscatter dependence on surface roughness, soil moisture and soil texture: Part I—Bare soil. *IEEE Transactions on Geoscience Electronics, 16*(4), 286–295.
- Ulaby, F. T., Fung, A. K., & Moore, R. K. (1981). *Microwave and remote sensing active and passive*. Norwood, MA: Artech House.
- Ulaby, F. T., Fung, A. K., & Moore, R. K. (1982). *Microwave and remote sensing: Active and passive: Surface scattering and emission theory*.
- Ulaby, F. T., Fung, A. K., & Moore, R. K. (1986). *Microwave and remote sensing active and passive*. Norwood, MA: Artech House.
- Wagner, W., & Scipal, K. (2000). Large-scale Soil moisture mapping in western Africa using the ERS scatterometer. *IEEE Transactions on Geoscience and Remote Sensing, 38*, 1777–1782.
- Wang, C., Qi, J., Moran, S., & Marsett, R. (2004). Soil moisture estimation in a semiarid rangeland using ERS-2 and TM imagery. *Remote Sensing of Environment, 90*, 178–189.
- Weiss, M., Baret, F., Smith, G. J., Jonckheere, I., & Coppin, P. (2004). Review of methods for in situ leaf area index (LAI) determination. Part II. Estimation of LAI, errors and sampling. *Agricultural and Forest Meteorology, 121*, 37–53.
- Woodhouse, I. H., & Hoekman, D. H. (2000). Determining land surface parameters from the ERS-1 wind scatterometer. *IEEE Transactions on Geoscience and Remote Sensing, 38*, 126–140.
- Zink, M. (2002). Introduction to the ASAR calibration/validation project. *The Envisat calibration review, Noordwijk (The Netherlands)*.
- Zribi, M., Le Hegarat-Masclé, S., Ottle, C., Kammoun, B., & Guerin, C. (2003). Surface soil moisture estimation from the synergistic use of the (multi-incidence and multi-resolution) active microwave ERS wind scatterometer and SAR data. *Remote Sensing of Environment, 86*, 30–41.